SIAM J. SCI. COMPUT.
Vol. 20, No. 2, pp. 534–552

A JACOBI WAVEFORM RELAXATION METHOD FOR ODEs*

J. SAND† AND K. BURRAGE‡

Abstract. A Jacobi waveform relaxation (WR) method for solving initial value problems for ordinary differential equations (ODEs) is presented. In each window the method uses a technique called *dynamic fitting* and a pair of continuous Runge–Kutta (RK) formulas to produce the initial waveform, after which a *fixed* number of waveform iterates are computed. The reliability and efficacy of the method are demonstrated numerically by applying it to qualitatively different problems for linear tridiagonal ODEs.

Key words. initial value problem, ordinary differential equation, pair of Runge–Kutta formulas, waveform relaxation

AMS subject classifications. 65L05, 65L06, 65Y05

PII. S1064827596306562

1. Introduction.

In the literature there seems to be a majority of negative results concerning parallel methods for ODEs. In the terminology of Gear [5], [6], *parallelism across the method* (being problem independent) only contributes to a low degree of parallelism, and some sort of *parallelism across the ODE system or a number of steps* (cf. [2]) is thus necessary in order to obtain a highly parallel method for large systems of ODEs. An example of parallelism across the system is the Jacobi version of the WR technique that was introduced in 1982 by Lelarasmee [12] and Lelarasmee, Ruehli, and Sangiovanni-Vincentelli [13]. Using the WR technique, certain problems arising from electrical network modelling can be solved extremely efficiently, whereas *in general* the actual rate of convergence of an iterative WR method may be very slow (cf. section 2).

Despite these negative results, we shall in the following present a highly parallel method and apply it to problems of the form

$$\dot{y} = Qy, \quad y(0) = (1, 0, \ldots, 0)^T \in \Re^d, \tag{1.1}$$

where Q is a real tridiagonal matrix with constants a, b, and c in its sub-, main, and superdiagonal, respectively.

The method will be based on a *fixed* number of Jacobi WR iterations, and the test problems (1.1) will include examples for which (more than a fixed number of) iterations would diverge on $[0, \infty)$, as well as examples where $\dot{y} = Qy$ is unstable, stiff or with highly oscillatory solutions. We have several reasons for choosing (1.1) as our class of test problems. First, an analytic expression for the solution as well as the waveforms can be found, enabling us to evaluate the error as well as the number of windows produced by the method. Second, the parameters a, b, and c make it possible to test the performance on ODEs with various types of solutions, and finally (1.1) may be regarded as a model for semidiscretized parabolic partial differential

*Received by the editors July 12, 1996; accepted for publication (in revised form) July 8, 1997; published electronically September 10, 1998.
http://www.siam.org/journals/sisc/20-2/30656.html

†Department of Computer Science, University of Copenhagen, Universitetsparken 1, DK–2100 Copenhagen, Denmark (datjs@diku.dk). This research was supported by the Danish Natural Science Research Council.

‡CIAMP, Department of Mathematics, University of Queensland, Brisbane 4072, Australia (kb@maths.uq.oz.au).

equations (PDEs) occurring in practice. Although our test problems are linear, all components of the numerical method are nevertheless defined for general nonlinear systems of ODEs!

In section 2, we discuss the WR technique. For general ODEs we bound the error of the waveforms by means of *arbitrary* vector norms, and for the test problems (1.1) we show that (even for normal matrices Q) the rate of converging Jacobi waveforms may be *far from linear* in the first many iterations. Hence, the usual choice of (constant) initial waveform should be improved, and in section 3 we describe the technique of *dynamic (linear least squares) fitting* used by our method to produce a time-varying initial waveform in each window. In section 4, we discuss the motivation for our choice of a *fixed* number of numerically computed waveforms, and in section 5 the integration formula is presented. The stepsize and window strategy is the subject of section 6, whereas section 7 contains the numerical results and some comments leading to the conclusions in section 8. In the appendix we list the technical proof of Theorem 2.2.

2. The WR technique. Let us first consider the WR technique applied to a *linear* system of ODEs:

$$\dot{y} = Ay + b, \quad t \geq t_0, \quad y(t_0) = y_0. \tag{2.1}$$

Splitting $A = M + N$, we obtain the waveforms $y^{(k)}$ defined by

$$\dot{y}^{(k)} = My^{(k)} + Ny^{(k-1)} + b, \;\; t \geq t_0, \;\; y^{(k)}(t_0) = y_0, \;\; k = 1, 2, \ldots, \tag{2.2}$$

where $y^{(0)}$ is the initial waveform.

Subtracting (2.2) from (2.1), we find that the error $e^{(k)} = y - y^{(k)}$ satisfies

$$\begin{aligned} e^{(k)}(t_1) &= \int_{t_0}^{t_1} e^{(t_1 - t_2)M} N e^{(k-1)}(t_2) dt_2 \\ &= \int_{t_0}^{t_1} \int_{t_0}^{t_2} \cdots \int_{t_0}^{t_k} \prod_{j=1}^{k} [e^{(t_j - t_{j+1})M} N] e^{(0)}(t_{k+1}) dt_{k+1} \cdots dt_3 dt_2; \end{aligned} \tag{2.3}$$

i.e., for all *finite* $t \geq t_0$ and any norm $\| \cdot \|$ on $\Re^d$,

$$\max_{\tau \in [t_0, t]} \|e^{(k)}(\tau)\| \leq C_k(t)(t - t_0)^k / k! \tag{2.4}$$

whenever

$$C_k(t) \geq \max \left\{ \left\| \prod_{j=1}^{k} (e^{(t_j - t_{j+1})M} N) e^{(0)}(t_{k+1}) \right\| : t_0 \leq t_{k+1} \leq t_k \leq \cdots \leq t_1 = t \right\}. \tag{2.5}$$

Clearly, one may choose

$$C_k(t) = \left(\max_{\tau \in [t_0, t]} \|e^{(t-\tau)M} N\| \right)^k \max_{\tau \in [t_0, t]} \|e^{(0)}(\tau)\| \tag{2.6}$$

and in this way obtain one of the error bounds in [17]. However, although the latter error bounds clearly demonstrate the superlinear convergence of the waveforms on any finite window, (2.4) and (2.5)—combined with the *estimation* of, e.g., $Ne^{(k-1)}$—may

be used to obtain more realistic error bounds. Likewise, the error bounds derived in case of nonlinear ODEs (see below) are often too pessimistic, and thus we will not use the error bounds to any great extent when we define our window strategy, for example.

For *nonlinear* systems of ODEs,

$$\dot{y} = f(t,y), \quad t \geq t_0, \;\; y(t_0) = y_0, \tag{2.7}$$

error bounds similar to (2.4), (2.6) have been shown by, e.g., Bjørhus [1] (see also [2], [3], and [7]), but the one-sided Lipschitz constant appearing in these bounds has only been defined in terms of an inner product! Since there are ODEs, which are dissipative only in norms *not* originating from inner products [21], the one-sided Lipschitz constant appearing in, e.g., [1] will for certain ODEs be larger than necessary (e.g., positive instead of negative). Therefore, we present error bounds in an *arbitrary* norm (using a result from [20]) in the following theorem.

THEOREM 2.1. *Consider the solution y of* (2.7) *and the waveforms $y^{(k)}$ defined by*

$$\dot{y}^{(k)} = F(t, y^{(k)}, y^{(k-1)}), \;\; t \geq t_0, \;\; y^{(k)}(t_0) = y_0, \;\; k = 1, 2, \ldots,$$

where $F(t,x,x) = f(t,x)\ \forall t, x$, and $y^{(0)}$ is the initial waveform. If $F(t,x,\cdot)$ satisfies the Lipschitz condition

$$\|F(t,x,u) - F(t,x,v)\| \leq L(t)\|u - v\| \ \forall t \geq t_0, u, v, x,$$

for some piecewise continuous $L(t)$, and $F(t,\cdot,x)$ satisfies

$$\|u - v - \delta[F(t,u,x) - F(t,v,x)]\| \geq (1 - \delta\mu(t))\|u - v\| \ \forall \delta \geq 0, t \geq t_0, u, v, x,$$

for some piecewise continuous $\mu(t)$, then

$$\|y(t) - y^{(k)}(t)\| \leq e_k(t), \tag{2.8}$$

where

$$\dot{e}_k(t) = \mu(t)e_k(t) + L(t)e_{k-1}(t), \;\; e_k(t_0) = 0, \;\; e_0(t) = \|y(t) - y^{(0)}(t)\|. \tag{2.9}$$

Proof. Theorem 2 in [20] bounds the difference between the exact and an approximate solution of an initial value problem. Let that problem be $\dot{z} = F(t, z, y^{(k-1)})$, $z(t_0) = y_0$. Then $y^{(k)}$ is the exact solution, and since y satisfies

$$\|\dot{y}(t) - F(t, y(t), y^{(k-1)}(t))\| \leq L(t)\|y(t) - y^{(k-1)}(t)\| \quad \forall t \geq t_0,$$

it follows from [20] that

$$\|y(t) - y^{(k)}(t)\| \leq e^{M(t)} \int_{t_0}^{t} L(\tau)e^{-M(\tau)}\|y(\tau) - y^{(k-1)}(\tau)\|d\tau,$$

where $M(t) = \int_{t_0}^{t} \mu(\tau)d\tau$. Using the above inequality to bound $\|y(t) - y^{(k)}(t)\|$ in terms of $e_0(\tau), \tau \in [0,t]$, one obtains (2.8). ∎

COROLLARY 2.1. *If the function μ in Theorem* 2.1 *is of constant sign (and nonzero) on $[t_0,t]$, then $e^{(k)}(t) = y(t) - y^{(k)}(t)$ satisfies*

$$\|e^{(k)}(t)\| \leq \left(\max_{\tau\in[t_0,t]} \frac{L(\tau)}{|\mu(\tau)|}\right)^k \left|1 - e^{M(t)} \sum_{j=0}^{k-1} \frac{(-M(t))^j}{j!}\right| \max_{\tau\in[t_0,t]} \|e^{(0)}(\tau)\|, \tag{2.10}$$

where

$$M(t) = \int_{t_0}^{t} \mu(\tau) d\tau.$$

Proof. By induction in k we find that $e_k(t)$ in (2.9) equals

$$e^{M(t)} \int_{t_0}^{t} L(t_2) \int_{t_0}^{t_2} L(t_3) \int_{t_0}^{t_3} \cdots \int_{t_0}^{t_k} L(t_{k+1}) e^{-M(t_{k+1})} e_0(t_{k+1}) dt_{k+1} \cdots dt_2$$

$$\leq \max_{\tau \in [t_0,t]} \|e^{(0)}(\tau)\| e^{M(t)} \int_{t_0}^{t} L(t_2) \int_{t_0}^{t_2} \cdots \int_{t_0}^{t_k} L(t_{k+1}) e^{-M(t_{k+1})} dt_{k+1} \cdots dt_2.$$

Let $I_k(L(t_{k+1}), e^{-M(t_{k+1})})$ denote the latter multiple integral. Since $-\mu(t_{k+1}) e^{-M(t_{k+1})}$ is of constant sign, from the generalized mean value theorem for integrals (cf., e.g., [11]) we obtain

$$I_k(L(t_{k+1}), e^{-M(t_{k+1})}) = I_{k-1}\left(\frac{L(t_{k+1,1})}{-\mu(t_{k+1,1})} L(t_k), e^{-M(t_k)} - 1 \right),\ t_{k+1,1} \in [t_0, t].$$

Once again $-\mu(t_k)(e^{-M(t_k)} - 1)$ is of constant sign, i.e.,

$$I_k(L(t_{k+1}), e^{-M(t_{k+1})}) = I_{k-2}\left(\frac{L(t_{k+1,2}) L(t_{k,1})}{\mu(t_{k+1,2}) \mu(t_{k,1})} L(t_{k-1}), e^{-M(t_{k-1})} - 1 + M(t_{k-1}) \right),$$

where $t_{k+1,2}, t_{k,1} \in [t_0, t]$. Proceeding in this way we obtain

$$I_k(L(t_{k+1}), e^{-M(t_{k+1})}) = \prod_{i=2}^{k+1} \left(\frac{L(t_{i,i-1})}{-\mu(t_{i,i-1})} \right) \left(e^{-M(t)} - \sum_{j=0}^{k-1} (-M(t))^j / j! \right),$$

where $t_{i,i-1} \in [t_0, t]\ \forall i$, and (2.10) follows from (2.8). ∎

Since $|1 - e^{M(t)} \sum_{j=0}^{k-1} \frac{(-M(t))^j}{j!}| = e^{\theta M(t)} |M(t)|^k / k!$ for some $\theta \in [0,1]$, (2.10) clearly demonstrates the superlinear convergence of the waveforms on any finite window (if μ exists, it can be chosen positive, of constant sign as required by the corollary), but if the error of $y^{(k-1)}$ is to be estimated, the following trivial formula may be of greater practical value in obtaining realistic *error estimates*:

$$\dot{e}^{(k)} = F(t, y, y) - F(t, y - e^{(k)}, y^{(k-1)}), \quad \text{where } y = y^{(k-1)} + e^{(k-1)}. \tag{2.11}$$

In regard to *windows of infinite length*, the work of Miekkala and Nevanlinna [16] shows that the errors $e^{(k)}$ in (2.3) satisfy

$$e^{(k)} = \mathcal{K}(e^{(k-1)}), \tag{2.12}$$

where the spectral radius of the integral operator $\mathcal{K}$ is

$$\rho(\mathcal{K}) = \max\{\rho((ixI - M)^{-1} N) \ :\ x \in \Re\}, \tag{2.13}$$

provided that the spectrum $\sigma(M)$ of M satisfies $\max \mathrm{Re}(\sigma(M)) < 0$. For the *static* iteration $v^{(k)} = -M^{-1} N v^{(k-1)}$, it is well known (cf., e.g., [4] or [18]) that the spectral radius $\rho(-M^{-1}N)$ can be very misleading in practice regarding the convergence rate,

and the use of pseudoeigenvalues for estimating or bounding $e^{(k)}$ in (2.3), (2.12) has been suggested in [19], [8], [15].

To see the difficulties in obtaining a useful error bound on infinite windows, let us consider the Jacobi WR technique applied to the model problems (1.1), i.e.,

$$\dot{y}^{(k)} = by^{(k)} + Ny^{(k-1)}, \quad y^{(k)}(0) = y_0 = (1, 0, \ldots, 0)^T \in \Re^d, \tag{2.14}$$

where N is a real tridiagonal matrix with constants a, 0, and c in its sub-, main, and superdiagonal, respectively. Choosing $y^{(0)}(t) \equiv y_0$ as the initial waveform, we have that the induction in k shows that

$$y^{(k)}(t) = [e^{bt}p_{k-1}(tN) + (N/(-b))^k(1 - e^{bt}p_{k-1}(-bt))]y_0,$$

where $p_{k-1}(x)$ is the truncated Maclaurin series $\sum_{j=0}^{k-1} x^j/j!$, i.e.,

$$y^{(k)}(\infty) = (N/(-b))^k y_0 \quad \text{if } b < 0. \tag{2.15}$$

In order to consider $y^{(k)}(\infty)$ and $y(\infty)$ in greater detail, we need the following result.

PROPOSITION 2.1. *If ac is nonzero then the matrix Q in* (1.1) *satisfies*

$$QV = V \operatorname{diag}\{b + 2\sqrt{ac}\cos(j\pi/(d+1)),\ j = 1, 2, \ldots, d\}, \tag{2.16}$$

where

$$V_{i,j} = (a/c)^{(i-1)/2}\sin(ij\pi/(d+1))$$

and

$$(V^{-1})_{i,j} = (2/(d+1))(c/a)^{(j-1)/2}\sin(ij\pi/(d+1)), \quad i, j = 1, 2, \ldots, d. \tag{2.17}$$

Proof. In some textbooks on PDEs, (2.16) can be seen to follow from the trigonometric identities

$$2\cos(jx)\sin(ijx) = \sin((i-1)jx) + \sin((i+1)jx), \quad i, j = 1, 2, \ldots, d.$$

(2.17) follows from

$$\sum_{j=1}^{d} \sin(kj\pi/(d+1))\sin(lj\pi/(d+1)) = ((d+1)/2)\delta_{k,l}, \tag{2.18}$$

which is easily proved by substituting $(e^{ix} - e^{-ix})/(2i)$ for $\sin x$. ∎

Applying Proposition 2.1 to Q in (1.1) and (with $b = 0$) to N in (2.15), we obtain the following theorem.

THEOREM 2.2. *For $b \le -2\sqrt{|ac|}$ $(ac \neq 0)$, the solution y of* (1.1) *goes to* 0 *as $t \to \infty$, whereas for $k \le d - 1$, the Jacobi WR iterates corresponding to $y^{(0)}(t) \equiv y_0$ satisfy*

$$[y^{(k)}(\infty)]_i = \begin{cases} 0 & \text{if } i > k+1 \text{ or } k - i \text{ is even,} \\ \left(\frac{2\sqrt{ac}}{-b}\right)^k \left(\frac{a}{c}\right)^{(i-1)/2} \alpha(i,k) & \text{otherwise,} \end{cases} \tag{2.19}$$

where

$$\alpha(i,k) = \begin{pmatrix} k+1 \\ (k+1-i)/2 \end{pmatrix} i/(2^k(k+1)) \ \sim\ \sqrt{\frac{8}{\pi e}}k^{-1} \tag{2.20}$$

if $k = 4m^2 - 1 \le d - 1$, $i = 2m$, and $m \to \infty$.

Proof. Being rather technical, the proof is moved to the appendix. ∎

In practice the ODE systems modelled by (1.1) (e.g., semidiscretized parabolic PDEs) are rather large, and thus one seldom iterates d times (or more). Therefore, (2.19) is of practical interest, and we note that the error of $(y^{(k)})_i$ at infinity consists of *three* factors: $(-2\sqrt{ac}/b)^k, (a/c)^{(i-1)/2}$, and $\alpha(i,k)$. The first of these factors is related to the *asymptotic rate of convergence*, i.e., $\rho(\mathcal{K})$ in (2.13). For $M = bI$, we note that $\rho(\mathcal{K}) = \rho(M^{-1}N)$, and thus (cf. Proposition 2.1) $\rho(\mathcal{K}) = |2\sqrt{ac}/b| \cos(\pi/(d+1))$. The second factor measures the *lack of symmetry of* Q, i.e., in some sense also the nonnormality of $M^{-1}N$ (the factor would be $(c/a)^{(i-1)/2}$ if we had $y(0) = (0,0,\ldots,0,1)^T$). The third factor shows that even when $b = -2\sqrt{ac}$ (i.e., $\rho(\mathcal{K}) < 1$) and $a = c$ (i.e., $M^{-1}N$ is normal) we may experience a convergence that is *far from linear* in the first many (fewer than d) iterations!

The lack of dissipativity as well as the many zero elements in the waveforms is of course due to the poor choice of initial waveform ($y^{(0)} \equiv (1,0,\ldots,0)^T$) and the decoupling of the system. If we want to use the Jacobi WR technique on reasonably large windows, the initial waveform should be allowed to vary with t! Finding $y^{(0)}$ by means of a block-Jacobi WR with a modest overlapping, e.g., (cf. [10]) will not change the number of zero elements significantly, and the same holds if we convolute the waveforms as in [19]. Being linear, the model problems (1.1) may be solved numerically by applying Krylov subspace techniques, e.g., (cf., e.g., section 6.3 in [2]), and since the problems usually occur in connection with the solution of parabolic PDEs, the multigrid technique proposed by Lubich and Ostermann in [14] seems like a good idea, but we are looking for a technique applicable to *general* (e.g., nonlinear) ODEs, and this is the subject of the next section.

3. The dynamic fitting technique. Assume (2.7), and set

$$y^{(0)}(t) = Bv(t), \tag{3.1}$$

where B is a constant $d \times n$ matrix ($d \gg n$) of rank n with $y(t_0)$ as its first coloumn. $v(t)$ is then found by minimizing $\|\dot{y}^{(0)} - f(t, y^{(0)})\|_2$ with respect to $\dot{v}(t)$, i.e., as the solution of the relatively small n-dimensional ODE system

$$\dot{v}(t) = (B^TB)^{-1}B^T f(t, Bv(t)), \quad v(t_0) = (1,0,\ldots,0)^T. \tag{3.2}$$

One of the properties of (3.1), (3.2) is that *any monotonicity in the ℓ_2-norm of the ODE system is inherited by* $y^{(0)}$:

$$(d/dt)\|y^{(0)}(t)\|_2^2 = 2y^{(0)}(t)^T f(t, y^{(0)}(t)).$$

As an example, $y^{(0)}(\infty) = 0$ in our model problem if $b \le -|a+c|$, since this implies that $Q + Q^T$ is negative definite (cf. Proposition 2.1).

In our tests we originally used $B = [\tilde{y}(t_0), (1,1,\ldots,1)^T]$, where $\tilde{y}(t_0)$ denotes the (numerically computed) value at the beginning of the window. In the first window we had $\tilde{y}(t_0) = (1,0,\ldots,0)^T$, and thus the initial waveform there obtained the form $y^{(0)}(t) = (\alpha(t), \beta(t), \beta(t), \ldots, \beta(t))^T$. $\alpha(t)$ resembled the first element of the solution $y(t)$, and $\beta(t)$ resembled the average of the remaining elements except in one of our test problems: In (1.1) with $(a,b,c) = (1,-20,100)$ and $d = 14$, $y^{(0)}(t)$ only resembled $y(t)$ for a very short time. As shown in Figure 3.1, the elements of $y(t)$ rapidly become very small, and so did the elements of $y^{(0)}(t)$, but unfortunately the small elements

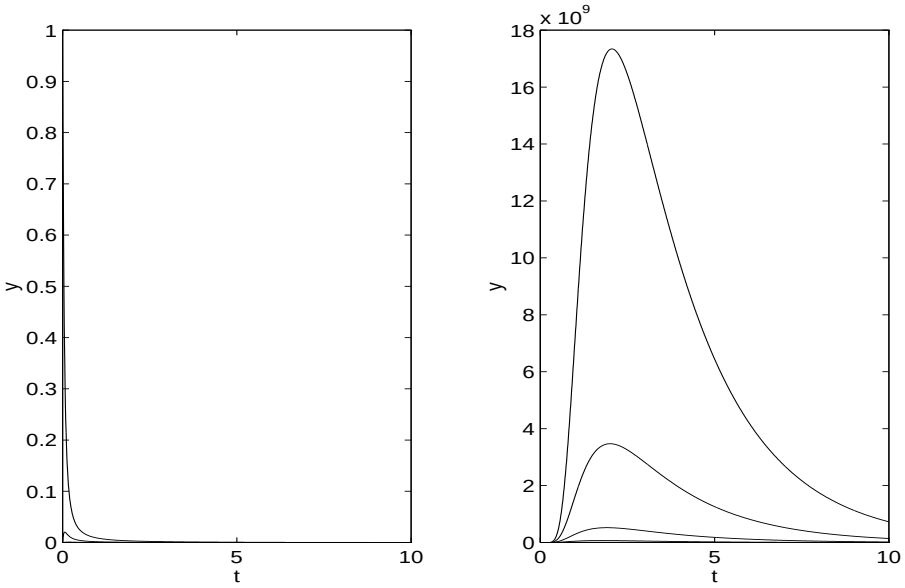

FIG. 3.1. *The solution of* (1.1) *with* $d = 14$, $(a, b, c) = (1, -20, 100)$, *and* $(a, b, c) = (100, -20, 1)$, *resp.*

of $y^{(0)}(t)$ resembled those of $y(t)$ *(in reverse order!)* so much that the numerical solution then started to trace the solution corresponding to $(a, b, c) = (100, -20, 1)$ instead (i.e., blew up as shown in Figure 3.1)!

Therefore, we changed B to the piecewise constant $d \times 1$ matrix $\tilde{y}(t_n)$ for $t \in [t_n, t_n + h)$, where h is the stepsize, and $\tilde{y}(t_n)$ is one of the most accurate estimates of $y(t_n)$ available when $y^{(0)}(t_n + h)$ is to be determined (in the notation of section 6, $\tilde{y} = Y_2^{(3)}$ in the first two steps of a window, and $\tilde{y} = Y_3^{(0)}$ otherwise). However, this *dynamic (least squares) fitting* was only used if the angle between $f(t_n, \tilde{y}(t_n))$ and $\tilde{y}(t_n)$ was close to π:

$$B^T f(t_n, B) < -0.9\|B\|_2 \|f(t_n, B)\|_2 \tag{3.3}$$

(otherwise $y^{(0)}(t_n + h)$ was set to $\tilde{y}(t_n)$). Condition (3.3) effectively prevented the method from using dynamic fitting until $y(t) = v_n(t)y(t_n)$, $t \in [t_n, t_n + h)$, became a reasonable model for some decreasing scalar-valued functions $v_n(t)$.

Let us conclude this section with an illustration of the following items.

(1) The analytic solution of (1.1) with $d = 5, (a, b, c) = (10, -20, 10)$ (i.e., Q is normal), and with $d = 5, (a, b, c) = (100, -20, 1)$ (i.e., $\rho(\mathcal{K}) < 1$, but $(\sqrt{|a/c|})^k \alpha(k + 1, k) = 5^k$).
The solutions are shown on the interval $[0, 10]$.

(2) The corresponding Jacobi waveforms $y^{(3)}$ when $y^{(0)} \equiv (1, 0, \ldots, 0)^T$.

(3) The corresponding window sizes used by our method (error tolerance = 0.002), when $y^{(0)} \equiv (1, 0, \ldots, 0)^T$ and when dynamic fitting is used in the case of (3.3).

(1), (2), and (3) are found in *rows* 1, 2, and 3, respectively, of Figure 3.2 below. Note that row 2 confirms (2.19) and that with dynamic fitting (solid line) the use of large windows is allowed much earlier than otherwise (dashed line). The stepsize is

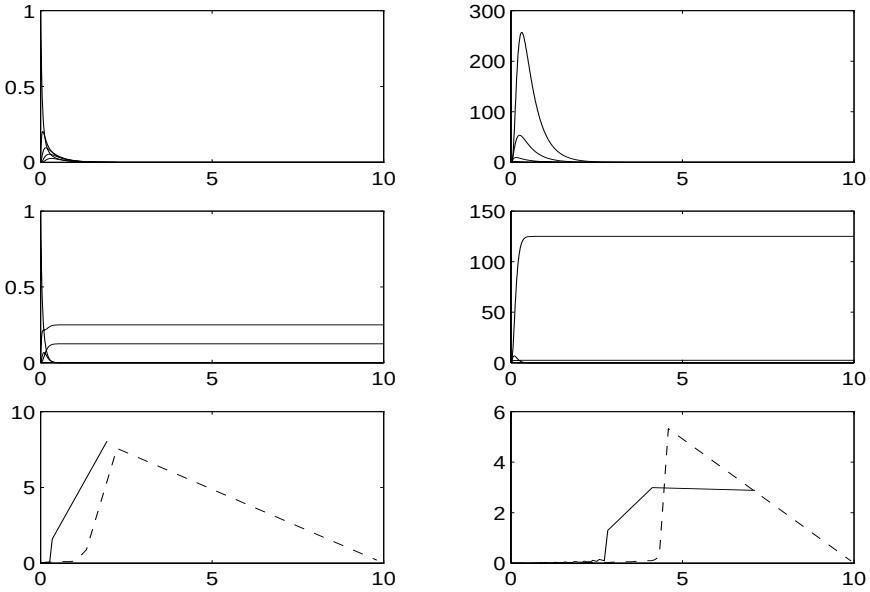

FIG. 3.2. *Illustration of analytic solutions, Jacobi waveforms and window sizes, as described in* (1)–(3) *above.*

kept *fixed* in each window, and thus some of the large windows are closed due to a no longer acceptable stepsize.

4. The number of computed waveforms. Although Corollary 2.1 states that the Jacobi waveforms converge at least superlinearly to the analytic solution on any finite window, *the accuracy of the numerical analogues is of course restricted by the order of the integration formula.* In other words, for a second-order formula the numerically computed $y^{(3)}(h), y^{(4)}(h), \ldots$, will all be equal to $y(h) + C_3 h^3 \frac{d^3}{(dt)^3} y(0) + \mathcal{O}(h^4)$, where h is the stepsize, and C_3 is the normalized error constant of the formula, provided that y is in $C^3[0, h]$. In the transient phase of a stiff system, the sizes of h and the windows will usually be so small that the second-order estimates of $y^{(3)}(t), y^{(4)}(t), \ldots$, do not differ significantly, and therefore our method is based on *only three Jacobi WR iterations*(!) (hoping that the fitting (3.1) will make $y^{(0)}$ and thus $y^{(3)}$ close to y in any "steady state type" of window). To illustrate that the second-order estimates of $y^{(3)}(t), y^{(4)}(t), \ldots$ differ very little in a window in the transient phase, we used the trapezoidal rule with $h = 10^{-3}$ to compute $y^{(k)}(t), k = 1, 2, \ldots, 6, t \in [0, 0.03]$, corresponding to (1.1) with $(a, b, c) = (10, -20, 10)$, and the order of Q equal to 10. The errors $\|y(t) - \mathit{computed}[y^{(k)}(t)]\|_\infty$ are shown in Figure 4.1. Note that with $h = 10^{-3}$, i.e., $\|C_3 h^3 \frac{d^3}{(dt)^3} y(0)\|_\infty = 1.2 \cdot 10^{-6}$, an error tolerance less than 10^{-5} seems reasonable, and the first window should therefore (cf. Figure 4.1) not include t-values larger than 0.013 (approximately), regardless of the number of waveform iterations!

5. The integration formula. In [9], parallelism across ordinary RK methods was examined. Among other results, it was shown that the order of the highly parallel "strictly diagonal" RK methods (in which each stage consists of an implicit Euler step) is at most 2. However, by replacing the implicit Euler by the trapezoidal rule, we

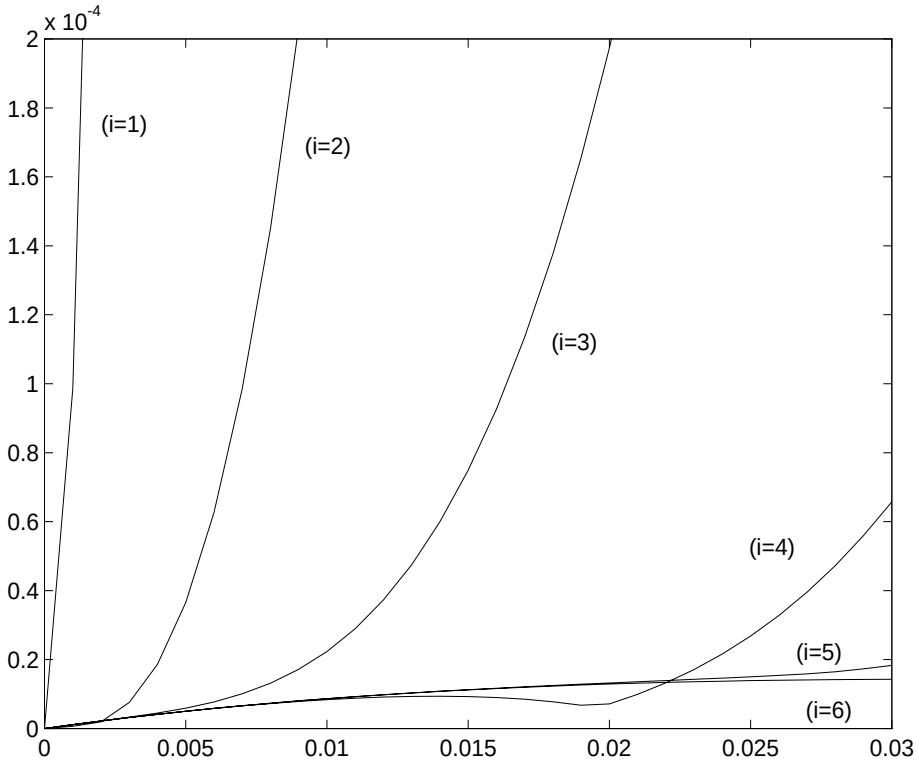

FIG. 4.1. *The max-norm error of the trapezoidal estimates of* $y^{(i)}(t), i = 1, 2, \ldots, 6$.

have derived an equally parallel (2,3)-pair of RK methods:

$$
\begin{array}{c|c|ccccc}
0 & 0 & & & & & \\
2/5 & 1/5 & 1/5 & & & & \\
3/4 & 3/8 & 0 & 3/8 & & & \\
8/9 & 4/9 & 0 & 0 & 4/9 & & \\
1 & 1/2 & 0 & 0 & 0 & 1/2 & \\
\hline
 & 1/2 & -25/70 & 6/7 & 0 & 0 & (2.order) \\
\hline
 & 1/2 & 0 & -24/5 & 54/5 & -11/2 & (3.order).
\end{array}
\tag{5.1}
$$

In order to use this method for estimating the value of a waveform at the point $t = t_n + h$, h being the stepsize, we need the value of the previous waveform at the points $t = t_n + \alpha h, \alpha \in \{0, 2/5, 3/4, 8/9, 1\}$. Assume that these values are known for the initial waveform. The values of the subsequent waveforms can then be estimated by using a continuous extension of the method (5.1). Let $\dot{y} = F(t, y)$ denote the ODE for which an estimate of $y(t_n + \alpha h)$ is needed, and let $\bar{y}_{n+\beta}$ denote the trapezoidal estimates

$$
\bar{y}_{n+\beta} = y_n + (\beta h/2)(F(t_n, y_n) + F(t_n + \beta h, \bar{y}_{n+\beta})),\ \beta \in \{2/5, 3/4, 8/9, 1\}. \tag{5.2a}
$$

The continuous extension of (5.1) that we chose can then be described as follows:

First-order estimate of $y(t_n + \alpha h)$ (order=2 for $\alpha = 1$).

$$
(1/2)y_n + ((15 - 40\alpha)/14)\bar{y}_{n+2/5} - ((4 - 20\alpha)/7)\bar{y}_{n+3/4}. \tag{5.2b}
$$

Second-order estimate of $y(t_n + \alpha h)$ (order=3 for $\alpha = 1$).

$$(5.2c)\quad \begin{aligned}(1/2)y_n + ((64 - 272\alpha + 144\alpha^2)/5)\bar{y}_{n+3/4} \\ -((243 - 1134\alpha + 648\alpha^2)/10)\bar{y}_{n+8/9} \quad +(12 - 59\alpha + 36\alpha^2)\bar{y}_{n+1}.\end{aligned}$$

As shown in the theorem below, the continuous method (5.2) is L-stable for $\alpha \in [0.198, 1]$.

THEOREM 5.1. *When applied to $\dot{y} = \lambda y$, the method* (5.2) *produces, respectively, the estimates $R_1(h\lambda)y_n$ and $R_2(h\lambda)y_n$, where the rational functions R_j, $j = 1, 2$, satisfy*

$$(5.3)\quad \begin{aligned}&|R_j(z)| \le 1 \text{ when } \operatorname{Re} z \le 0, \quad \alpha \in [0.198, 1], \quad \text{and} \\ &\quad R_j(z) \to 0 \text{ for } |z| \to \infty.\end{aligned}$$

Proof. After some formula manipulation one finds that

$$R_1(z) = (40 - (23 - 40\alpha)z)/((5 - z)(8 - 3z))$$

and

$$R_2(z) = (144 - (190 - 144\alpha)z + (83 - 190\alpha + 72\alpha^2)z^2)/((8 - 3z)(9 - 4z)(2 - z)).$$

Hence, $R_1(z)$ and $R_2(z)$ go to 0 as $|z| \to \infty$. Furthermore, since they are analytic in an open set containing $\{z : \operatorname{Re} z \le 0\}$, it follows from the maximum modulus principle that $\max\{|R_j(z)| : \operatorname{Re} z \le 0\} = \max\{|R_j(ix)| : x \in \Re\}$, $j = 1, 2$. The equations $R_j(ix)R_j(-ix) = 1$, $j = 1, 2$, however, are equivalent to

$$x^2(9x^2 + p_1(\alpha)) = 0 \text{ and } 4x^4(36x^2 + p_2(\alpha)) = 0,$$

respectively, where

$$p_1(\alpha) = -240 + 1840\alpha - 1600\alpha^2 \ge 0 \quad \text{for } \alpha \in [0.15, 1]$$

and

$$p_2(\alpha) = -1140 + 7885\alpha - 12013\alpha^2 + 6840\alpha^3 - 1296\alpha^4 \ge 0 \text{ for } \alpha \in [0.198, 2.44].$$

For $\alpha \in [0.198, 1]$ the moduli of $R_j(ix)$ are thus at most 1, and the theorem follows.

6. The stepsize and window strategy. As mentioned in section 4, our method is based on three Jacobi WR iterations. However, in the *beginning* of each window we iterate *four times* in order to obtain a third-order estimate from our (2,3)-pair of RK formulas. This way we hope to find a constant stepsize that is appropriate at least in the beginning of the window. Let

$$Y_p^{(k)}(t_n), \quad k = 0, 1, \ldots, 4, \quad p = 2, 3,$$

denote the pth-order estimates of the waveforms $y^{(k)}$ at t_n, and let t_0 be the starting point of the window (i.e. the $Y_p^{(k)}(t_0)$'s are identical). For a given error tolerance $\varepsilon > 0$, the first stepsize of the window is then determined such that the following conditions are satisfied:

$$(6.1)\quad \|Y_3^{(4)}(t_0 + h) - Y_2^{(3)}(t_0 + h)\|_\infty \in (\varepsilon/20, \varepsilon/2],$$

and if $\max_{k\in[1,4]} \|Y_3^{(k)}(t_0+h) - Y_3^{(k-1)}(t_0+h)\|_\infty > \varepsilon/2$ then

$$\|Y_3^{(k)}(t_0+h) - Y_3^{(k-1)}(t_0+h)\|_\infty \le \beta^{k-1}\|Y_3^{(1)}(t_0+h) - Y_3^{(0)}(t_0+h)\|_\infty, \tag{6.2}$$

for $k = 1, 2, \ldots, 4$, where

$$\beta < 1 \text{ and } \beta^3\|Y_3^{(1)}(t_0+h) - Y_3^{(0)}(t_0+h)\| \le (1-\beta)\varepsilon/2.$$

Clearly, (6.1) has to do with the principal local truncation error of the second-order formula, whereas (6.2) tries to govern the accuracy of the waveform $y^{(3)}$ according to

$$\begin{aligned}\|y(t_0+h) - y^{(3)}(t_0+h)\|_\infty &\lesssim \sum_{k=4}^{\infty} \|y^{(k)}(t_0+h) - y^{(k-1)}(t_0+h)\|_\infty \\ &\lesssim \left(\sum_{k=4}^{\infty} \beta^{k-1}\right) \|Y_3^{(1)}(t_0+h) - Y_3^{(0)}(t_0+h)\|_\infty \lesssim \frac{\varepsilon}{2}.\end{aligned}$$

Having determined the stepsize, an implementation may now benefit from the parallelism of the Jacobi WR and the RK method, until the window has to be closed due to a no longer appropriate stepsize (apart from this, a window is of course limited in size by the entire integration interval and the window used in the previous sweep). In our tests, we used the following condition to indicate that a window should be closed *in the kth sweep* ($k = 1, 2,$ *or* 3) due to a no longer appropriate stepsize

$$\delta = \max\{2^{k-3} yerror(k),\ \|Y_3^{(k)}(t_n) - Y_2^{(k)}(t_n)\|_\infty\} \notin (\varepsilon/100, \varepsilon/2], \tag{6.3a}$$

where $t_n = t_0 + nh$, and $yerror(k)$ equals

$$\begin{aligned}\min\ \{&\|Y_3^{(k)}(t_n) - Y_3^{(k-1)}(t_n)\|_\infty, \\ &h\|F(t_n, Y_3^{(k)}(t_n), Y_3^{(k)}(t_n)) - F(t_n, Y_3^{(k)}(t_n), Y_3^{(k-1)}(t_n))\|_\infty\}.\end{aligned} \tag{6.3b}$$

In δ the term $\|Y_3^{(k)}(t_n) - Y_2^{(k)}(t_n)\|_\infty$ clearly measures the accuracy of the second-order formula, whereas $yerror(k)$ combines an estimate of $\|y(t_n) - y^{(k-1)}(t_n)\|_\infty$ with a bound on the *change* in $y(t) - y^{(k)}(t)$ from $t = t_n$ to $t = t_n + h$ if h is small (cf. (2.11)):

$$\begin{aligned}&\|[y(t_n+h) - y^{(k)}(t_n+h)] - [y(t_n) - y^{(k)}(t_n)]\|_\infty \\ &\approx h\|F(t_n, y(t_n), y(t_n)) - F(t_n, y^{(k)}(t_n), y^{(k-1)}(t_n))\|_\infty.\end{aligned}$$

Since $y^{(k+1)}$ is not estimated until the $(k+1)$st sweep, it is difficult to produce a more well-founded estimate of the error of $y^{(k)}$ in the kth sweep, and as we shall see in the next section, the mixed condition (6.3) actually seems to work quite well in many situations.

7. Numerical results. As described in sections 3 to 5, our method consists of using an L-stable highly parallel (2,3)-pair of RK formulas to compute a second-order estimate of the Jacobi waveform $y^{(3)}$, where $y^{(0)}$ is defined in section 3 (and computed by means of the third-order formula). In each window a constant stepsize is used for computing each of the components of $y^{(3)}$, and the sizes of steps and windows are determined by (6.1)–(6.3).

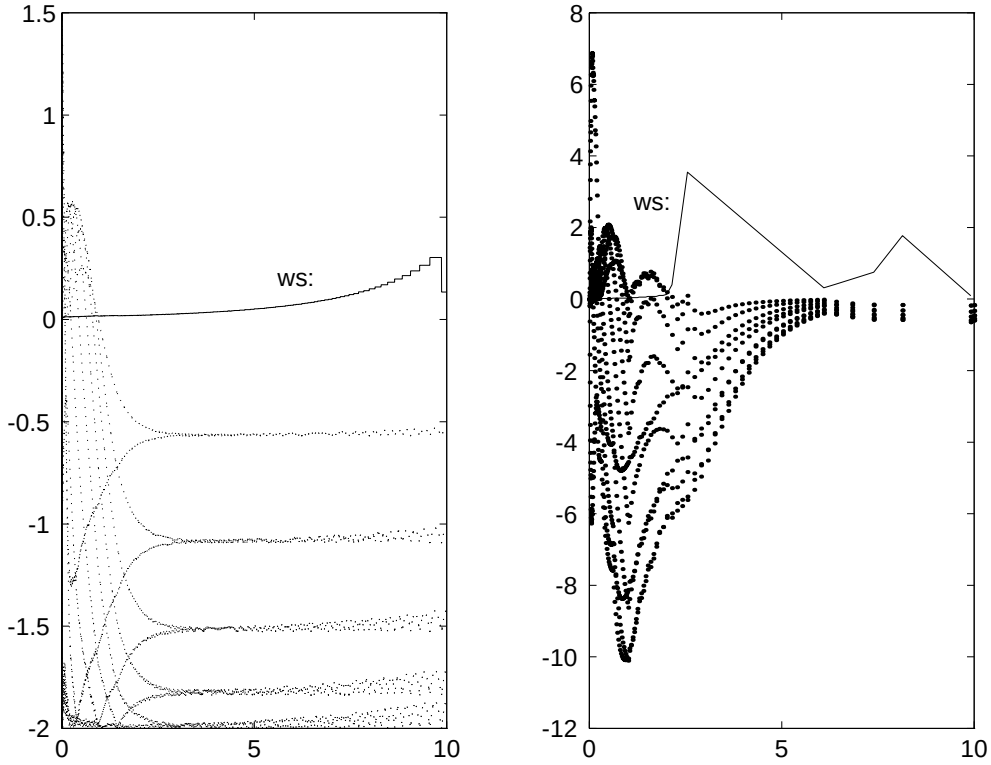

FIG. 7.1. *Window sizes (ws) and* 10^5 *times the error of* $y^{(3)}$ *in the analytic and the numerical case, respectively.*

Since the choice of windows generally has been considered one of the most difficult tasks in using the WR technique, we wanted in particular to test this part of the method. Therefore, we developed a program that estimates those windows $W_i = [\hat{t}_i, \hat{t}_{i+1}]$, $i = 0, 1, \ldots$, that satisfy (ε = the error tolerance)

$$\hat{t}_{i+1} = \max\{t \,:\, \hat{t}_i \le t \le T \text{ and } \|y(t) - y^{(3)}(\hat{t}_i, t)\|_\infty \le \varepsilon\}, \tag{7.1}$$

where $\hat{t}_0 = 0$ and $[0, T]$ is the entire integration interval. $y^{(3)}(\hat{t}_i, \cdot)$ is the *analytic* Jacobi waveform obtained by three WR iterations from a piecewise constant initial waveform $y^{(0)}(\cdot)$ ($y^{(0)}(t) = y(\hat{t}_0)$ on $[\hat{t}_0, \hat{t}_1)$, and $y^{(0)}(t) = y^{(3)}(\hat{t}_{i-1}, \hat{t}_i)$ on $[\hat{t}_i, \hat{t}_{i+1})$ for $i \ge 1$). Since the error of $y^{(3)}(\hat{t}_i, \hat{t}_i)$ is *equal* to ε, W_i may for certain problems be of length 0, and in that case we will denote the number of "analytically determined windows" by ∞.

In Figure 7.1 the first of the two plots shows the analytic window sizes (solid line) and 10^5 times the components of the analytic error $y(t) - y^{(3)}(\hat{t}_i, t)$, corresponding to the problem (1.1) with error tolerance $\varepsilon = 2 \cdot 10^{-5}$, dimension $d = 10$, and parameters $(a, b, c) = (10, -20, 10)$. On the integration interval [0,10], the number of analytic windows turns out to be 267.

The second plot in Figure 7.1 shows the sizes of the windows used by our numerical method (solid line) and 10^5 times the error components. In the beginning most of the windows are one-step windows, but at approximately $t = 2.5$ a window

slightly larger than 3.5 t-units appears. Since the stepsize is fixed in each window, the latter window is closed when the error estimates indicate that the stepsize is too small. The number of "numerical windows" in [0,10] is 110, and since three of these windows shrunk during the sweeps, the total number of steps in each sweep is 199, 163, and 131, respectively. A desirable property of the numerical method is that

- the errors as well as the number of windows and steps are *unchanged* if the parameters a, b, c, T^{-1}, and h_0^{-1} (where $h_0 = T\sqrt{\varepsilon/2000}$ is our estimate of the first stepsize to be used) are *scaled* by the same number.

Hence, $|ac|$ has been set to 100 in all our tests, and this leaves d, ε, T, a, b, and $sign(ac)$ as our test parameters.

Since the eigenvalues of Q in (1.1) are $b + 2\sqrt{ac}\cos(j\pi/(d+1)),\ j = 1, 2, \ldots, d$, we have decided on the following choices of a, b, c, and T:

$$\begin{aligned} &a \in \{\pm 1, \pm 10, \pm 100\}, \\ &(b, c, T) \in \{(-20, 100/a, 10), (2, 100/a, 0.1), (-2, -100/a, 1)\}. \end{aligned} \tag{7.2}$$

Let us illustrate the analytic solution of these 18 problems in the case $d = 5$. Since our method also has the following desirable property,

- the numerical (as well as the analytic) solutions of (7.2) corresponding to $(a, c) = -(\alpha, \beta)$ and $(a, c) = (\alpha, \beta)$ are the same, except that every second component differs in sign,

we only show the solution of the problems (7.2) corresponding to $a > 0$ in Figure 7.2.

All our calculations were performed in MATLAB, and we examined four different cases of (dimension, local error tolerance)

- $(d, \varepsilon) \in \{(5, 2 \cdot 10^{-3}), (5, 2 \cdot 10^{-5}), (14, 2 \cdot 10^{-3}), (50, 2 \cdot 10^{-3})\}$.

For each of the 72 pairs of (problem, case) we now list five rows, the contents of which are (respectively)

(i) the number of "analytic" windows W_i (cf. (7.1)) and windows produced by the numerical method, respectively;
(ii) the number of multistep windows in sweep 1, the number of windows shrinking from sweep 1 to sweep 3, and the number of multistep windows in sweep 3;
(iii) the number of steps in each of the three sweeps;
(iv) the maximal max-norm error and the minimal (disregarding the zero error at $t = 0$);
(v) the maximum of the mixed absolute-relative error $\|y(t) - (\textit{the second-order estimate})\|_\infty / \max\{1, \|y(t)\|_\infty\}$.

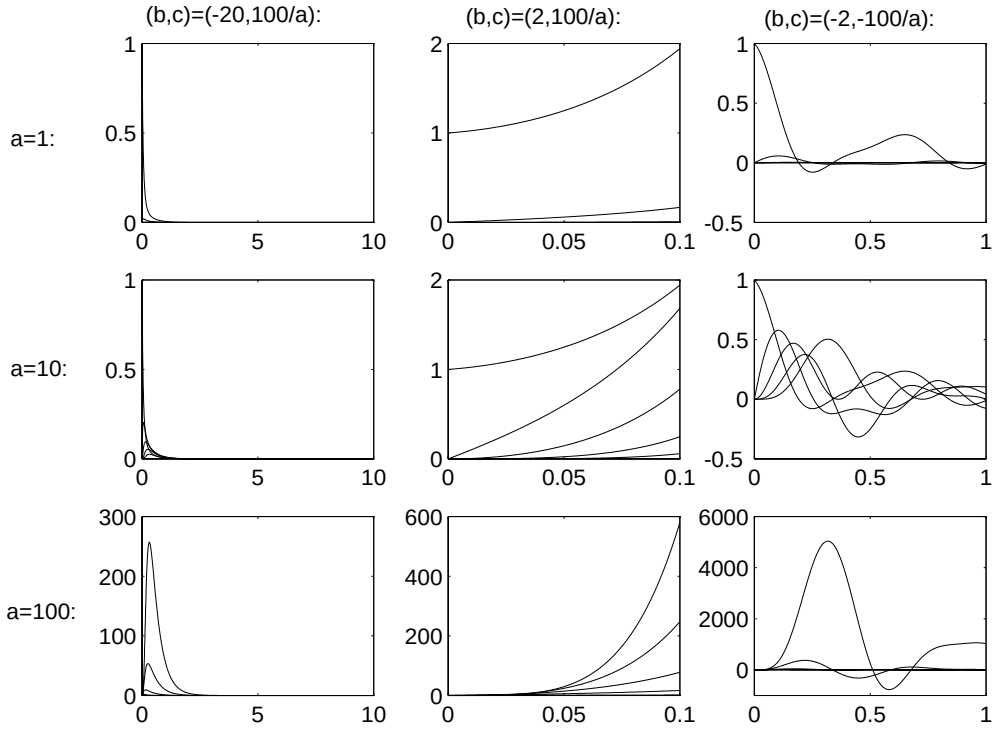

FIG. 7.2. *Analytic solutions (t,y) corresponding to* (7.2).

Case 1 ($d = 5,\ \varepsilon = 2 \cdot 10^{-3}$):

a	$c = 100/a$ $(b, T) = (-20, 10)$	$c = 100/a$ $(b, T) = (2, 0.1)$	$c = -100/a$ $(b, T) = (-2, 1)$
± 1	∞ 15 5 2 5 76 46 32 $1.9 \cdot 10^{-3}$ $6.1 \cdot 10^{-6}$ $1.9 \cdot 10^{-3}$	∞ 8 0 0 0 8 8 8 $5.9 \cdot 10^{-3}$ $3.6 \cdot 10^{-5}$ $3.0 \cdot 10^{-3}$	∞ 67 13 7 7 86 80 74 $1.0 \cdot 10^{-2}$ $3.2 \cdot 10^{-5}$ $1.0 \cdot 10^{-2}$
± 10	19 12 1 0 1 23 23 23 $2.3 \cdot 10^{-3}$ $7.0 \cdot 10^{-5}$ $2.3 \cdot 10^{-3}$	∞ 9 0 0 0 9 9 9 $7.6 \cdot 10^{-3}$ $1.8 \cdot 10^{-4}$ $3.9 \cdot 10^{-3}$	∞ 42 0 0 0 42 42 42 $1.4 \cdot 10^{-2}$ $1.5 \cdot 10^{-4}$ $1.4 \cdot 10^{-2}$
± 100	∞ 251 56 51 17 2725 639 282 $2.5 \cdot 10^{-2}$ $2.8 \cdot 10^{-5}$ $6.8 \cdot 10^{-3}$	∞ 98 0 0 0 98 98 98 $3.0 \cdot 10^{-1}$ $2.0 \cdot 10^{-4}$ $4.6 \cdot 10^{-3}$	∞ 708 0 0 0 708 708 708 $3.8 \cdot 10^{-1}$ $2.0 \cdot 10^{-4}$ $4.2 \cdot 10^{-3}$

Case 2 ($d = 5,\ \varepsilon = 2 \cdot 10^{-5}$):

a	$c = 100/a$ $(b, T) = (-20, 10)$	$c = 100/a$ $(b, T) = (2, 0.1)$	$c = -100/a$ $(b, T) = (-2, 1)$
± 1	∞ 95 14 7 8 254 168 122 $6.7 \cdot 10^{-5}$ $3.8 \cdot 10^{-7}$ $6.7 \cdot 10^{-5}$	∞ 31 0 0 0 31 31 31 $4.8 \cdot 10^{-4}$ $1.3 \cdot 10^{-6}$ $2.5 \cdot 10^{-4}$	∞ 237 0 0 0 237 237 237 $7.2 \cdot 10^{-4}$ $1.2 \cdot 10^{-6}$ $7.2 \cdot 10^{-4}$
± 10	115 71 9 6 5 226 225 92 $6.9 \cdot 10^{-5}$ $1.3 \cdot 10^{-6}$ $6.9 \cdot 10^{-5}$	∞ 37 0 0 0 37 37 37 $5.1 \cdot 10^{-4}$ $2.3 \cdot 10^{-6}$ $2.6 \cdot 10^{-4}$	∞ 198 0 0 0 198 198 198 $6.6 \cdot 10^{-4}$ $2.1 \cdot 10^{-6}$ $6.6 \cdot 10^{-4}$
± 100	∞ 1075 264 256 46 10870 1485 1134 $1.2 \cdot 10^{-3}$ $1.8 \cdot 10^{-7}$ $3.1 \cdot 10^{-4}$	∞ 455 0 0 0 455 455 455 $1.5 \cdot 10^{-2}$ $1.1 \cdot 10^{-6}$ $2.7 \cdot 10^{-4}$	∞ 2954 0 0 0 2954 2954 2954 $2.0 \cdot 10^{-2}$ $1.1 \cdot 10^{-6}$ $2.5 \cdot 10^{-4}$

Case 3 ($d = 14,\ \varepsilon = 2 \cdot 10^{-3}$):

a	$c = 100/a$ $(b, T) = (-20, 10)$	$c = 100/a$ $(b, T) = (2, 0.1)$	$c = -100/a$ $(b, T) = (-2, 1)$
± 1	∞ 15 5 2 5 82 52 37 $4.3 \cdot 10^{-3}$ $2.7 \cdot 10^{-4}$ $4.3 \cdot 10^{-3}$	∞ 8 0 0 0 8 8 8 $5.9 \cdot 10^{-3}$ $3.6 \cdot 10^{-5}$ $3.0 \cdot 10^{-3}$	∞ 48 9 3 8 131 71 70 $1.7 \cdot 10^{-3}$ $3.2 \cdot 10^{-5}$ $1.7 \cdot 10^{-3}$
± 10	49 23 7 6 4 322 133 50 $1.0 \cdot 10^{-2}$ $6.6 \cdot 10^{-4}$ $1.0 \cdot 10^{-2}$	∞ 9 0 0 0 9 9 9 $7.6 \cdot 10^{-3}$ $1.8 \cdot 10^{-4}$ $3.9 \cdot 10^{-3}$	∞ 39 0 0 0 39 39 39 $1.0 \cdot 10^{-2}$ $1.5 \cdot 10^{-4}$ $1.0 \cdot 10^{-2}$
± 100	$(\max \|y(t)\|_\infty > 10^{10})$	∞ 243 0 0 0 243 243 243 $2.7 \cdot 10^{1}$ $7.4 \cdot 10^{-4}$ $7.3 \cdot 10^{-3}$	$(\max \|y(t)\|_\infty > 10^{12})$

Case 4 ($d = 50,\ \varepsilon = 2 \cdot 10^{-3}$):

a	$c = 100/a$ $(b, T) = (-20, 10)$	$c = 100/a$ $(b, T) = (2, 0.1)$	$c = -100/a$ $(b, T) = (-2, 1)$
± 1	∞ 15 5 2 5 82 52 37 $4.3 \cdot 10^{-3}$ $2.1 \cdot 10^{-4}$ $4.3 \cdot 10^{-3}$	∞ 8 0 0 0 8 8 8 $5.9 \cdot 10^{-3}$ $3.6 \cdot 10^{-5}$ $3.0 \cdot 10^{-3}$	∞ 48 9 3 8 131 71 70 $1.7 \cdot 10^{-3}$ $3.2 \cdot 10^{-5}$ $1.7 \cdot 10^{-3}$
± 10	49 23 7 6 4 322 133 50 $1.1 \cdot 10^{-2}$ $6.6 \cdot 10^{-4}$ $1.1 \cdot 10^{-2}$	∞ 9 0 0 0 9 9 9 $7.6 \cdot 10^{-3}$ $1.8 \cdot 10^{-4}$ $3.9 \cdot 10^{-3}$	∞ 39 0 0 0 39 39 39 $1.0 \cdot 10^{-2}$ $1.5 \cdot 10^{-4}$ $1.0 \cdot 10^{-2}$
± 100	$(\max \|y(t)\|_\infty > 10^{44})$	∞ 243 0 0 0 243 243 243 $2.7 \cdot 10^{1}$ $2.0 \cdot 10^{-4}$ $7.3 \cdot 10^{-3}$ (Errors for t$\in \{h, 0.1\}$!)	$(\max \|y(t)\|_\infty > 10^{33})$

For $d = 50, (a, b) = (\pm 100, 2)$, we only computed (in Maple) the max-norm errors after the first and the last step, since computation of the *exact* solution values required more than 50 digits of accuracy! Actually we also solved problems with $(b, T) = (-200, 1)$, but we have not included these results in the schemes above, since it is natural to *expect* good results from a Jacobi WR method when Q resembles a diagonal matrix. To show that our method actually *did* perform well on these problems, we just list the results corresponding to $(d, \varepsilon) = (50, 2 \cdot 10^{-3})$:

$c = 100/a$ $a \in \{\pm 1, \pm 10\}$	$c = 100/a$ $a = \pm 100$	$c = -100/a$ $a \in \{\pm 1, \pm 10\}$	$c = -100/a$ $a = \pm 100$
1 4 2 0 2 22 22 22 $1.7 \cdot 10^{-3}$ $1.3 \cdot 10^{-5}$ $1.7 \cdot 10^{-3}$	5 11 1 0 1 14 14 14 $2.4 \cdot 10^{-3}$ $4.4 \cdot 10^{-5}$ $2.4 \cdot 10^{-3}$	1 4 2 0 2 22 22 22 $1.7 \cdot 10^{-3}$ $2.3 \cdot 10^{-5}$ $1.7 \cdot 10^{-3}$	5 11 1 0 1 14 14 14 $2.4 \cdot 10^{-3}$ $4.2 \cdot 10^{-5}$ $2.4 \cdot 10^{-3}$

In the preceding schemes, we have for each (d, ε) listed the results corresponding to 18 different test problems, and in order to comment on these results we now group the problems according to the scheme below:

a	$(b, c) = (-20, 100/a)$	$(b, c) = (2, 100/a)$	$(b, c) = (-2, -100/a)$
± 1	C	B	D
± 10	E		
± 100	A		A

Our comments on the numerical results are as follows.

Problems of group A. Due to an almost explosive growth of the exact solution (cf. Figure 7.2), these problems seem rather unrealistic for dimension $d > 5$ (say), and

since only the result for $(b, c) = (-20, 100/a)$ shows a "waste" of steps (of approximately 75%), the results for group A seem acceptable.

Problems of group B. Although group B contains problems for which the ODE is unstable ($b = 2$), and where $\rho(\mathcal{K})$ in (2.13) is larger than 1 ($b = \pm 2$), no windows shrank from sweep 1 to sweep 3, and the local(!) error tolerance ε was only exceeded by a factor larger than 13.5 in the highly oscillatory case $b = -2, \varepsilon = 2 \cdot 10^{-5}$ (cf. Figure 7.2).

Problems of group C. The results demonstrate a window shrinkage of factor 1.4 (approximately) in each sweep. Since we only make three sweeps *and* avoid the blowing up illustrated in Figure 3.1, the results for group C seem satisfactory.

Problems of group D. Somehow the solutions for $d = 5$ are less accurate than those for $d = 14$ and $d = 50$ (if ε is set to $2 \cdot 10^{-5}$, the mixed absolute-relative error for $d \in \{14, 50\}$ becomes $1.7 \cdot 10^{-4}$). For $\varepsilon = 2 \cdot 10^{-5}$ all windows were one-step windows (for $d \in \{14, 50\}$ 208 steps were used), whereas for $\varepsilon = 2 \cdot 10^{-3}$ and $d \in \{14, 50\}$ 23% of the steps are seen to be "wasted."

Problems of group E. In all our runs (including one with $(d, \varepsilon) = (50, 2 \cdot 10^{-5})$), the *accuracy* was acceptable, and for $(d, \varepsilon) = (50, 2 \cdot 10^{-5})$ the percentage of "wasted" steps was only 12.8%. However, the wastage of 70% of the steps in the cases $d = 14$ or $d = 50$ and $\varepsilon = 2 \cdot 10^{-3}$ may not be quite satisfactory. The total number of steps used for $d = 14$ and $d = 50$ turned out to be the same.

8. Concluding remarks. As indicated by the comments concluding section 7, the results of this relatively simple highly parallel method have made us optimistic regarding the possibility of developing a parallel general-purpose code (including higher-order formulas and maybe more sophisticated techniques).

By applying our method to a number of problems with qualitatively different solutions (cf. Figure 7.2), we find that our method seems quite *reliable* (although we do not claim to have made any complete test of the method!). Furthermore, the use of Jacobi waveform relaxation, the integration formula (5.2), and constant stepsize in each window make the method *highly parallel*. As to the *efficacy*, we noted in the beginning of this paper that iterative WR methods often converge very slowly (*if* they converge! See also Theorem 2.2). Our method, however, only uses a *fixed* number of iterations (three) to produce a waveform of the same order of accuracy as the limit waveform (if it exists), and yet the number of windows seems reasonably small (at least when compared with the number of "analytic" windows). We believe this is mainly due to the *dynamic fitting* (cf. Figure 3.2) and an appropriate *window strategy* (6.3).

Appendix (Proof of Theorem 2.2). Let D denote the diagonal matrix

$$\operatorname{diag}\{(a/c)^{(i-1)/2} \ : \ i = 1, 2, \ldots, d\},$$

and let S be the matrix $[\sin(ij\pi/(d+1))]_{i,j}$. From (2.15) and Proposition 2.1 it then follows that

$$y^{(k)}(\infty) = \frac{2}{d+1} D\, S \operatorname{diag}\left\{ \left(\frac{2\sqrt{ac}}{-b} \right)^k \cos(i\pi/(d+1))^k \ : \ i \right\} S\, D^{-1} y_0;$$

i.e.,

$$[y^{(k)}(\infty)]_i = \left(\frac{2\sqrt{ac}}{-b} \right)^k \left(\frac{a}{c} \right)^{(i-1)/2} \beta(i, k),$$

where

$$\beta(i,k) = \frac{2}{d+1}\sum_{j=1}^{d} \sin(ij\pi/(d+1))\cos(j\pi/(d+1))^k \sin(j\pi/(d+1)).$$

Using the trigonometric identity $\cos x \sin y = (\sin(x+y)+\sin(x-y))/2$ k times, we find that

$$\cos(j\pi/(d+1))^k \sin(j\pi/(d+1)) = 2^{-k}\sum_{m=0}^{k} \left(\begin{array}{c} k \\ m \end{array} \right) \sin((2m+1-k)j\pi/(d+1)),$$

and thus from (2.18)

$$\begin{aligned}\beta(i,k) &= \frac{2^{1-k}}{d+1}\sum_{m=0}^{k} \left(\begin{array}{c} k \\ m \end{array} \right) \sum_{j=1}^{d} \sin(ij\pi/(d+1))\sin((2m+1-k)j\pi/(d+1)) \\ &= 2^{-k}\sum_{m=0}^{k} \left(\begin{array}{c} k \\ m \end{array} \right) \mathrm{sign}(2m+1-k)\delta_{i,|\,2m+1-k\,|}.\end{aligned}$$

For $i > k+1$ or $k-i$ even, $\beta(i,k)$ is clearly 0, and otherwise

$$\beta(i,k) = 2^{-k}\left[\left(\begin{array}{c} k \\ (k+i-1)/2 \end{array} \right) - \left(\begin{array}{c} k \\ (k-i-1)/2 \end{array} \right) \right] = \alpha(i,k).$$

This proves (2.19). As to (2.20), one may use Stirling's formula (or probability arguments) to find that

$$\begin{aligned}\alpha(i,k) &\sim \sqrt{\tfrac{2}{\pi k}}(e^{-(i-1)^2/(2k)} - e^{-(i+1)^2/(2k)}) \\ &= \sqrt{\tfrac{2}{\pi k e}}(e^{(i-1)/k} - e^{-(i+1)/k}) \sim \sqrt{\tfrac{8}{\pi e}}k^{-1}\end{aligned}$$

when $i^2 = k+1$ and $k \to \infty$.

Acknowledgment. Several suggestions from one of the referees helped us to improve the presentation of our results.

REFERENCES

[1] M. Bjørhus, *A note on the convergence of discretized dynamic iteration*, BIT, 35 (1995), pp. 291–296.
[2] K. Burrage, *Parallel and Sequential Methods for Ordinary Differential Equations*, Oxford Univ. Press, Oxford, 1995.
[3] P. Chartier, *Parallélisme dans la résolution numerique des problèmes de valeur initiale pour les équations différentielles ordinaires et algébriques*, Ph.D. Thesis, Univ. of Rennes, France, 1993.
[4] J. L. M. van Dorsselaer, J. F. B. M Kraaijevanger, and M. N. Spijker, *Linear stability analysis in the numerical solution of initial value problems*, Acta Numerica, (1993), pp. 199–237.
[5] C. W. Gear, *The potential for parallelism in ordinary differential equations*, in Computational Mathematics, S. Fatunla, ed., Boole Press, Dublin, 1987, pp. 33–48.
[6] C. W. Gear, *Parallel methods for ordinary differential equations*, Calcolo, 25 (1989), pp. 1–20.
[7] K. J. in 't Hout, *On the convergence of waveform relaxation methods for stiff nonlinear ordinary differential equations*, Appl. Numer. Math., 18 (1995), pp. 175–190.

[8] Z. Jackiewicz, B. Owren, and B. Welfert, *Convergence Analysis of Waveform Relaxation Methods Using Pseudospectra*, Preprint, Dept. of Math. Sciences, The Norwegian Inst. of Technology, 1996.
[9] K. R. Jackson and S. P. Nørsett, *The potential for parallelism in Runge–Kutta methods. Part* 1*: RK Formulas in standard form*, SIAM J. Numer. Anal., 32 (1995), pp. 49–82.
[10] R. Jeltsch and B. Pohl, *Waveform relaxation with overlapping splittings*, SIAM J. Sci. Comput., 16 (1995), pp. 40–49.
[11] D. S. Jones and D. W. Jordan, *Introductory Analysis, Vols.* I *and* II, John Wiley and Sons, New York, 1969.
[12] E. Lelarasmee, *The Waveform Relaxation Method for the Time Domain Analysis of Large Scale Nonlinear Dynamical Systems*, Ph.D. thesis, Univ. of California, Berkeley, 1982.
[13] E. Lelarasmee, A. Ruehli and A. Sangiovanni-Vincentelli, *The waveform relaxation method for time domain analysis of large scaled integrated circuits*, IEEE Trans. on CAD of IC and Sys., 1 (1982), pp. 131–145.
[14] C. Lubich and A. Ostermann, *Multi-grid dynamic iteration for parabolic equations*, BIT, 27 (1987), pp. 216–234.
[15] A. Lumsdaine and D. Wu, *Spectra and pseudospectra of waveform relaxation operators*, SIAM J. Sci. Statist. Comput., 18 (1997), pp. 286–304.
[16] U. Miekkala and O. Nevanlinna, *Convergence of dynamic iteration methods for initial value problems*, SIAM J. Sci. Statist. Comput., 8, (1987), pp. 459–482.
[17] O. Nevanlinna, *Remarks on Picard-Lindelöf iteration. Part* I, BIT, 29 (1989), pp. 328–346.
[18] S. C. Reddy and L. N. Trefethen, *Stability of the method of lines*, Numer. Math., 62 (1992), pp. 235–267.
[19] M. W. Reichelt, J. K. White, and J. Allen, *Optimal convolution SOR acceleration of waveform relaxation with application to parallel simulation of semiconductor devices*, SIAM J. Sci. Comput., 16 (1995), pp. 1137–1158.
[20] J. Sand and S. Skelboe, *Stability of backward Euler multirate methods and convergence of waveform relaxation*, BIT, 32 (1992), pp. 350–366.
[21] M. N. Spijker, *On the relation between stability and contractivity*, BIT, 24 (1984), pp. 656–666.